PET Imaging of Monoamine Oxidase B in Peripheral Organs in Humans

Joanna S. Fowler, PhD[1]; Jean Logan, PhD[1]; Gene-Jack Wang, MD[2]; Nora D. Volkow, MD[2]; Wei Zhu, PhD[3]; Dinko Franceschi, MD[2]; Naomi Pappas, MS[2]; Richard Ferrieri, PhD[1]; Colleen Shea, MS[1]; Victor Garza, MS[1]; Youwen Xu, MS[1]; Robert R. MacGregor, BS[1]; David Schlyer, PhD[1]; S. John Gatley, PhD[2]; Yu-Shin Ding, PhD[1]; and David Alexoff, BS[1]

[1]Chemistry Department, Brookhaven National Laboratory, Upton, New York; [2]Medical Department, Brookhaven National Laboratory, Upton, New York; and [3]Department of Applied Mathematics and Statistics, State University of New York Stony Brook, Stony Brook, New York

Monoamine oxidase (MAO) regulates neurotransmitter concentration in the brain and is also an important detoxifying enzyme in peripheral organs. It occurs in 2 subtypes, MAO A and MAO B. Their relative ratios in different organs are variable, depending on the particular organ and species, making it difficult to extrapolate measures from animals to humans. The purpose of this study was to investigate the feasibility of imaging MAO B in peripheral organs in humans with PET. **Methods:** Nine healthy subjects (7 males, 2 females; mean age ± SD, 37 ± 7 y) received 2 dynamic PET studies of the torso area 2 h apart with ^{11}C-L-deprenyl and deuterium-substituted ^{11}C-L-deprenyl (^{11}C-L-deprenyl-D2). Time–activity curves for heart, lungs, liver, kidneys, and spleen and arterial plasma input were measured for each study. The uptake at plateau and the incorporation quotient (IQ = uptake/plasma input) as well as model terms K_1 (which is a function of blood flow) and k_3 and λk_3 (which are kinetic terms proportional to MAO B) were compared to identify organs that showed reduced values with deuterium substitution (deuterium isotope effect) characteristic of MAO B. In addition, a sensitivity analysis compared the 2 tracers with respect to their ability to quantify MAO B. **Results:** Heart, lungs, kidneys, and spleen showed a robust deuterium isotope effect on uptake, IQ, k_3, and λk_3. The arterial plasma input function was significantly larger for ^{11}C-L-deprenyl-D2 than for ^{11}C-L-deprenyl. Liver time–activity curves were not affected by deuterium substitution and model terms could not be estimated. In organs showing an isotope effect, λk_3 showed the rank order: kidneys ≥ heart > lungs = spleen. A sensitivity analysis showed that ^{11}C-L-deprenyl-D2 is a better index of MAO activity than ^{11}C-L-deprenyl. **Conclusion:** This study demonstrates that (a) the deuterium isotope effect is useful in assessing the binding specificity of labeled deprenyl to peripheral MAO B; (b) MAO B can be visualized and quantified in the heart, lungs, kidneys, and spleen but not in the liver; (c) with the exception of the liver, which cannot be measured, MAO B activity is highest in the kidneys and heart; and (d) quantitation in organs having high levels of MAO B is improved by the use of ^{11}C-L-deprenyl-D2, similar to prior studies on the brain. This study indicates that ^{11}C-L-deprenyl-D2 will be useful for measuring the effects of different variables, including tobacco smoke exposure on MAO B activity in peripheral organs in humans.

Key Words: PET; monoamine oxidase B; peripheral organs

J Nucl Med 2002; 43:1331–1338

Monoamine oxidases (MAOs) are flavin-containing enzymes occurring in the brain and in peripheral organs. They oxidize amines from both endogenous and exogenous sources, thereby regulating the concentration of neurotransmitter amines as well as many xenobiotics. MAO occurs in 2 subtypes, MAO A and MAO B. These are different gene products and have different inhibitor and substrate specificities (*1*). MAO A preferentially oxidizes norephinephrine and serotonin and is selectively inhibited by clorgyline (*2*), whereas MAO B preferentially breaks down benzylamine and phenethylamine and is selectively inhibited by L-deprenyl (*3*). Both forms oxidize dopamine (*4*). Their relative ratios in different organs are variable, depending on the particular organ and species, making it difficult to extrapolate measures from animals to humans.

Medical interest in MAO has historically focused on the brain, beginning with the serendipitous discovery that a MAO inhibitor drug that was being used to treat tuberculosis improved mood in these patients (*5*,*6*). This led to the development of MAO inhibitor drugs to treat diseases of central origin, including depression (*7*), Parkinson's disease (*8*), and Alzheimer's disease (*9*). However, peripheral MAO represents a vast and complex mechanism for regulating circulating catecholamines and amines from exogenous sources and for regulating blood pressure (*10*,*11*). In this sense, peripheral MAO plays a protective role. This is well illustrated by reports of hypertensive crises occurring when individuals taking MAO inhibitor drugs ingest foods containing tyramine, a vasoactive chemical compound occurring in many fermented foods (*11*). In fact, a common warning in the prescription of many drugs is to avoid coadministration with MAO inhibitor drugs.

Received Dec. 26, 2001; revision accepted Jun. 11, 2002.

For correspondence contact: Joanna S. Fowler, PhD, Chemistry Department, Brookhaven National Laboratory, Upton, NY 11973.

E-mail: fowler@bnl.gov

The metabolites from MAO-catalyzed oxidation are also of medical interest. MAO generates a molecule of hydrogen peroxide for each molecule of amine that is oxidized. There is evidence that hydrogen peroxide may play a role in cell signaling and function (*12*). Additionally, MAO-generated hydrogen peroxide is a potential source of oxidative damage via the iron-catalyzed generation of hydroxyl radicals (*13*). MAO B catalyzes the conversion of 1-methyl-4-phenyl-1,2,3,6-tetrahydropyridine (MPTP) to 1-methyl-4-phenylpyridinium ion (MPP^+), which is toxic to dopaminergic neurons in brain, leading to Parkinson's disease. MAO B inhibitor drugs such as L-deprenyl prevent MPTP-induced toxicity (*14*). Although most studies of MPTP toxicity have focused on the brain, there is speculation that species differences in toxicity may be due to species differences in peripheral MAO B, which would oxidize MPTP to MPP^+, which cannot cross the blood–brain barrier (*15,16*).

We have developed methods for imaging MAO A and B in the human brain using PET and ^{11}C-labeled irreversible inhibitors clorgyline and L-deprenyl, and we have used these methods to investigate the effect of drugs, tobacco smoke, and aging on MAO A and B in the human brain (*17–21*). We report the extension of this approach to investigate the feasibility of imaging MAO in peripheral organs in humans. We undertook this study to assess the feasibility of measuring the effects of tobacco smoke, which we have shown to inhibit MAO in human brain (*18,19*), as well as the effects of other substances on MAO activity in peripheral organs. This is relevant because peripheral inhibition of MAO could contribute to smoking toxicity. We used the deuterium isotope effect (*22,23*) to identify organs where the image clearly represents MAO activity, and we applied compartmental modeling to quantify MAO activity in organs showing an isotope effect similar to that of prior studies in the human brain (*23*). This study focused specifically on the measurement of peripheral MAO B in humans using paired studies of ^{11}C-L-deprenyl and deuterium-substituted ^{11}C-L-deprenyl (^{11}C-L-deprenyl-D2).

MATERIALS AND METHODS

Subjects

These studies were approved by the Institutional Review Board at Brookhaven National Laboratory, and written informed consent was obtained from each subject after the procedures had been explained. Nine healthy subjects (7 males, 2 females; mean age ± SD, 37 ± 7 y) were recruited by newspaper advertisements and word-of-mouth. Exclusion criteria included medical illness that may affect monoamine levels or monoamine metabolism; a history of drug or alcohol abuse including nicotine; the current use of herbal medicines or medications that may affect monoamine levels or monoamine metabolism; a positive urine screen for drugs of abuse. All 9 volunteers completed both sets of scans, although only the data from 8 were used because of movement during the scan in 1 subject, which degraded the image and prevented region-of-interest (ROI) placement.

PET Scans

PET scans were run on a whole-body, high-resolution positron emission tomograph (HR+; Siemens/CTI, Knoxville, TN; 4.5 × 4.5 × 4.8 mm at center of field of view) in 3-dimensional dynamic acquisition mode. Subjects were positioned with their torso in the tomograph and their arms overhead and outside of the camera with a goal of having both the heart and the kidneys in the field of view. A transmission scan was obtained with a ^{68}Ge rotating rod source before each emission scan to correct for attenuation before each radiotracer injection. Catheters were placed in an antecubital vein for radiotracer injection and in the radial artery for blood sampling. ^{11}C-L-Deprenyl and ^{11}C-L-deprenyl-D2 were prepared as described (*24,25*). Each subject received both tracers with a time interval of 2–3 h between injections. Six of the subjects had ^{11}C-L-deprenyl first and 3 of the subjects had ^{11}C-L-deprenyl-D2 first. The dose of ^{11}C-L-deprenyl or ^{11}C-L-deprenyl-D2 averaged 240.5 ± 33.3 MBq (6.5 ± 0.9 mCi); the specific activity was about 9,250 MBq/μmol (250 mCi/μmol) at the time of injection. Sequential PET scans were obtained immediately after injection for a total of 60 min with the following timing: 6 × 20-s frames; 4 × 60-s frames; 2 × 120-s frames; 10 × 300-s frames. During the PET scan, arterial blood samples were automatically withdrawn (Ole Dick Instruments, Hvidovre, Denmark), every 2.5 s for the first 2 min, then every minute from 2 to 6 min, and then at 8, 10, 15, 20, 30, 45, and 60 min. Each arterial blood sample was centrifuged, the plasma was pipetted, and the radioactivity was counted. Plasma samples at 1, 5, 10, 20, 30, 45, and 60 min were analyzed for ^{11}C-L-deprenyl (or ^{11}C-L-deprenyl-D2) as described (*26*).

ROIs

Emission data were corrected for attenuation and reconstructed using filtered backprojection. For the purpose of region identification for the ^{11}C-L-deprenyl (or ^{11}C-L-deprenyl-D2) scans, time frames from dynamic images taken from 0 to 60 min were summed. Planes were added in groups of 2 to obtain 16–30 planes for ROI placement. The number of planes was determined by subject positioning (i.e., whether or not both the heart and kidneys were in the field of view). ROIs were drawn directly on PET scans using an atlas for reference (*27*). ROIs for the following areas were obtained for the purpose of this analysis: heart, lungs, liver, kidneys, stomach, and spleen. Regions for each organ were identified on 2 or 3 planes and the weighted average was obtained. Right and left lung and right and left kidney regions were averaged. For the kidneys, the region placement was made on the cortex because the medulla was devoid of radioactivity. The regions were then projected to the dynamic scans to obtain the concentration of ^{11}C versus time and expressed as a percentage of the total injected dose per cm^3.

Kinetic Analysis

Time–activity curves for ^{11}C-L-deprenyl and ^{11}C-L-deprenyl-D2 were compared to identify organs that showed the reduction in binding rate characteristic of the deuterium isotope effect. PET time–activity data for ^{11}C-L-deprenyl and ^{11}C-L-deprenyl-D2 for these organs as well as the time–activity data from arterial plasma were used to calculate an incorporation quotient (IQ), which is equal to the average uptake at plateau/plasma integral over 60 min and normalizes organ uptake for the amount of radiotracer in the plasma. The uptake (% dose/mL) was obtained by examining the time–activity curves and averaging the time points that occurred during the plateau phase. The plateau occurred at slightly different times for the different organs: 12.5–60 min for lungs, liver, and

heart; 17.5–60 min for spleen; and 9–60 min for kidneys. A 3-compartment model was used to calculate K_1, the plasma-to-organ transfer constant, which is related to blood flow; k_2, which is related to the transfer of tracer from the organ to plasma; and k_3, the kinetic constant controlling the rate of binding to MAO B. MAO B concentration was not determined directly but, rather, inferred from the model term k_3. However, because estimates of k_2 and k_3 are highly correlated, a bias can occur in the estimation of k_3. This is particularly problematic in regions of high MAO B concentration in which k_2 may be underestimated, leading to an underestimation of k_3 and of the inferred relative enzyme concentration. Using the combination model parameter λk_3, the correlation problem is reduced because λk_3 depends on the ratio k_3/k_2. We also previously found that reproducibility in test–retest studies is improved using λk_3 rather than k_3 as the model parameter for comparison (*28*). The combination parameter, λk_3, is used as an index of MAO B. λ is defined as K_1/k_2 and is independent of blood flow (*29*). We have previously used a similar model to estimate functional MAO B activity in the human brain (*23*).

For each organ, the residual blood volume in the organ (*30*) was applied as a correction factor and model terms for the lung were also corrected for 70% air in the volume of interest (*31*). The residual blood volumes that were used for the spleen, heart, lungs, and kidneys were 25%, 7%, 5%, and 7%, respectively. Spillover was minimized by fitting the data using times >1.5 min, for which the blood radioactivity is substantially less than the peak value that occurs generally at times <1 min. Partial volume is more difficult to correct and could introduce errors if misapplied. Because the organs studied should have the same partial-volume effects across subjects, we accept this as a bias but one that contributes a similar amount to each subject.

Sensitivity of Model Parameters

The ability to accurately estimate λk_3 depends on its value relative to K_1. When $\lambda k_3 \gg K_1$ (or equivalently $k_3 \gg k_2$), uptake depends primarily on K_1 and is relatively insensitive to changes in k_3 or λk_3. Using Ki (the influx constant (*32*)) given by $K_1k_3/(k_2 + k_3)$, as a measure of uptake, the sensitivity of Ki to changes in λk_3 can be calculated in terms of the normalized derivative $\partial Ki/\partial\lambda k_3(\lambda k_3/Ki)$.

Because $\partial Ki/\partial\lambda k_3(\lambda k_3/Ki) = 1 - \lambda k_3/(K_1 + \lambda k_3)$, the maximum value is 1. As λk_3 increases relative to K_1, the sensitivity decreases. To illustrate this, a plot of $\partial Ki/\partial\lambda k_3(\lambda k_3/Ki)$ versus λk_3 was generated for K_1 values of 0.25, 0.50, 1.0, 1.5, 2.0, and 2.5 mL/min/mL.

Statistical Analysis

The plasma input function, the IQ, and the model terms K_1, k_2, k_3, λk_3, and k_3/k_2 for heart lungs, kidneys, and spleen for ^{11}C-L-deprenyl and ^{11}C-L-deprenyl-D2 were compared using paired-samples t tests. We realize that there is a multiple-comparison concern, but it is not feasible to do a good correction for so many tests. We provided the P values (2-sided) for those considered significantly different so the readers could make a better judgment. We examined the rank order of the IQ, K_1, and λk_3 using a repeated-measures general linear model to examine the homogeneity of the ROIs. (Only the IQ was calculated for the liver because no model fit to the data could be obtained.) There are 4 ROIs: heart, lungs, kidneys, and spleen. Eight subjects are included in the analysis, but there are only 23 observations available because of the fact that all organs were not visualized on all subjects. The analysis was performed using SAS PROC GLM (SAS Institute Inc., Cary, NC).

RESULTS

It was not possible to image both heart and kidneys in the same session for all of the subjects. Kidney images were obtained for 7 subjects and heart (and lung) images were obtained for 5 subjects. The liver was in the field of view for 8 subjects and the spleen was in the field of view for 6 subjects. Summed images of ^{11}C-L-deprenyl and ^{11}C-L-deprenyl-D2 from 7 to 60 min for 1 subject are shown in Figure 1. There is a large reduction in uptake with ^{11}C-L-deprenyl-D2 relative to ^{11}C-L-deprenyl that can be seen for the kidneys and a less apparent reduction for the heart, lungs, and spleen because they have significantly less accumulation than the kidneys.

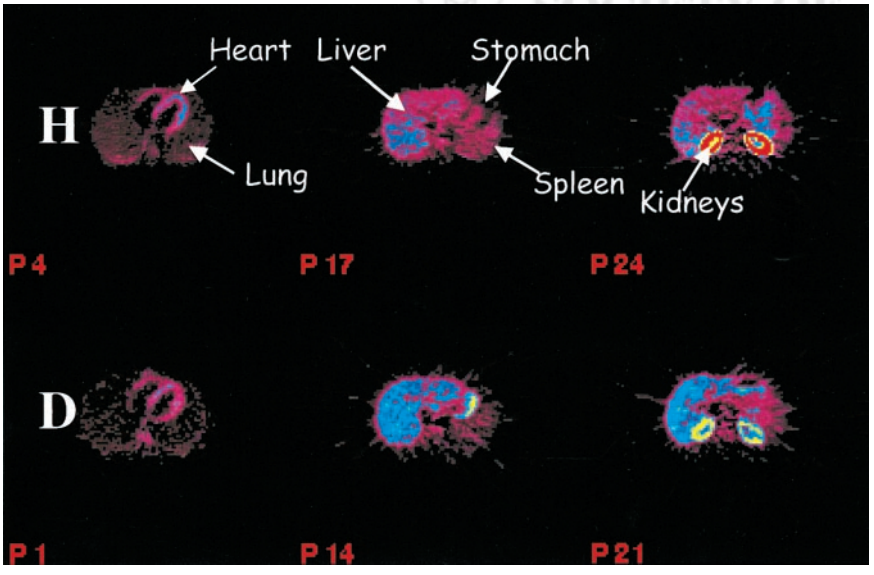

FIGURE 1. Summed images (from 7 to 60 min) for 1 subject for ^{11}C-L-deprenyl (H) (top row) and ^{11}C-L-deprenyl-D2 (D) (bottom row). Planes from left to right show heart and lungs (planes 4 and 1); liver, stomach, and spleen (planes 17 and 14); and kidneys (planes 24 and 21). Note reduced accumulation of ^{11}C with ^{11}C-L-deprenyl-D2. Rainbow color scale is used.

Time–activity curves for kidneys, heart, lungs, spleen, and liver for 1 subject are shown in Figure 2. The highest uptake occurred in the kidneys. For the kidneys, the uptake curves differed for the 2 tracers with ^{11}C-L-deprenyl typically peaking at around 5 min and leveling off at about 5–10 min. In contrast, ^{11}C-L-deprenyl-D2 showed a very rapid initial rise and fall, peaking at around 5 min with a plateau at around 10 min at about half the value of ^{11}C-L-deprenyl. The pattern in the heart was similar to that of the kidney with a significant reduction in ^{11}C concentration at the plateau with deuterium substitution. The ^{11}C concentration at the plateau was considerably lower for the heart than for the kidneys for both tracers. For the lungs there was a very rapid uptake with a peak at 0.5 min followed by a rapid clearance and a plateau at around 12 min. Deuterium substitution reduced the concentration of ^{11}C at the plateau in the lungs. The time–activity curves for the spleen were somewhat similar to those for the lungs with a rapid uptake peaking at 1–2 min followed by a rapid washout and a plateau at around 10 min. The ^{11}C concentration at the plateau was reduced with deuterium substitution. For the liver there was a slower uptake for both tracers with a peak around 10 min and a plateau thereafter for both tracers.

The input function (radiotracer concentration vs. time) was significantly higher for ^{11}C-L-deprenyl-D2 than for ^{11}C-L-deprenyl (8,621 ± 1,406 vs. 11,507 ± 1,406 Bq/mL × min [233 ± 38 vs. 311 ± 38 nCi/mL × min]; paired t, –7.6; $P < 0.0001$). Time–activity curves and the corresponding integrals are shown for 1 subject in Figures 3A and 3B, respectively.

The average values for the IQ and the model terms K_1, k_2, k_3, λk_3, and the k_3/k_2 ratio are shown in Table 1 for each tracer. K_1, which is related to blood flow, did not differ between ^{11}C-L-deprenyl and ^{11}C-L-deprenyl-D2 except for a small effect in the kidney ($P = 0.04$). In contrast, the IQ, k_3, λk_3, and k_3/k_2 were significantly different for the 2 radiotracers for the heart, lungs, kidneys, and spleen with ^{11}C-L-deprenyl being 1.8–5.7 times higher than ^{11}C-L-deprenyl-D2 ($P < 0.003$). Average values for K_1 and for λk_3 are shown in the bar plot in Figures 4A and 4B.

Similar to prior studies on the brain (*23*), the sensitivity of λk_3 to changes in MAO B concentration is degraded as the value of λk_3 increases, and this is exacerbated with smaller values of K_1 (Fig. 5). Thus, the sensitivity to differences in MAO B concentration is greater for ^{11}C-L-deprenyl-D2 than for ^{11}C-L-deprenyl because the values of λk_3 are smaller (Fig. 4B). In addition, though the IQ and λk_3 are highly correlated for all of the organs for both ^{11}C-L-deprenyl and ^{11}C-L-deprenyl-D2 ($P < 0.02$), there is a danger in general

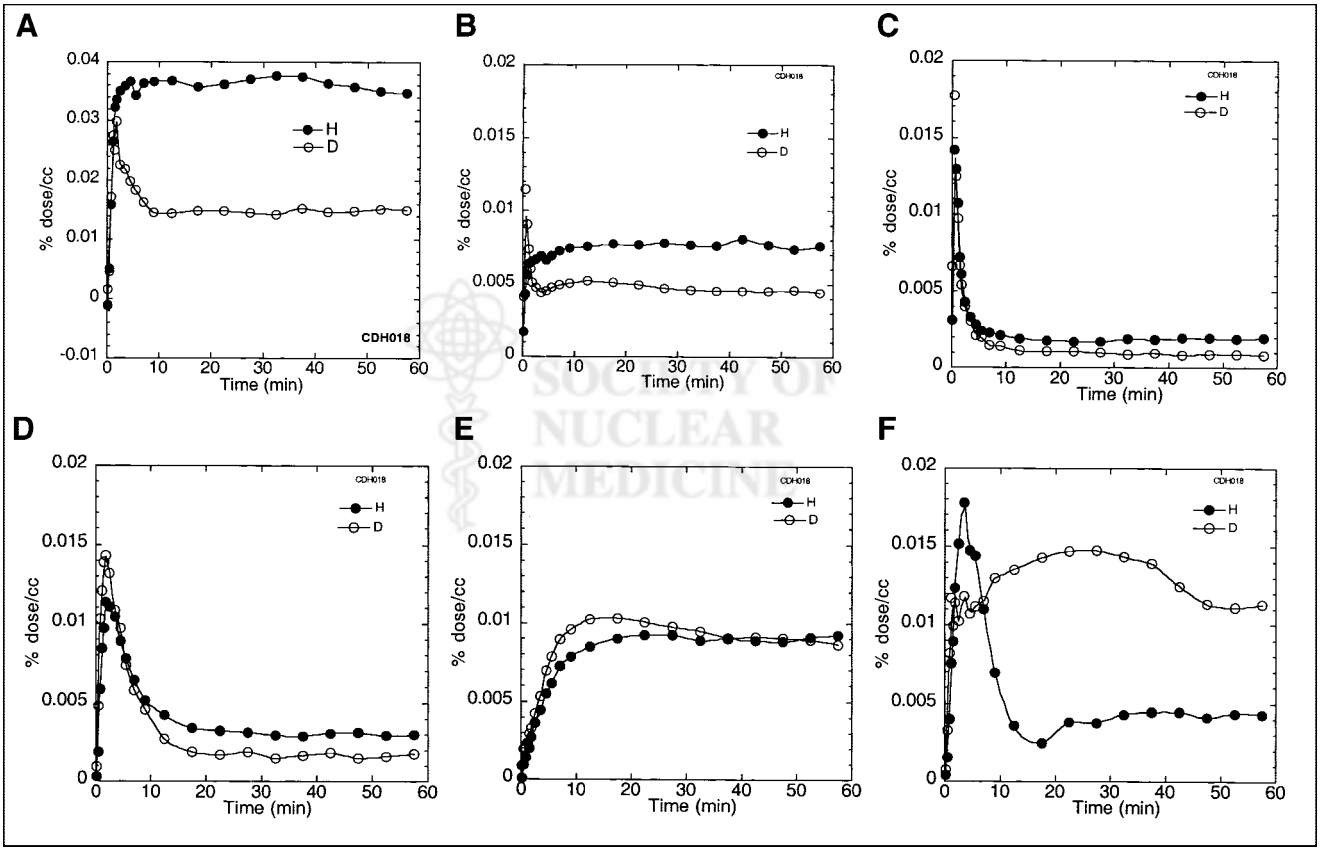

FIGURE 2. Time–activity curves for 1 subject for kidneys (A), heart (B), lungs (C), spleen (D), liver (E), and stomach (F) after injection of ^{11}C-L-deprenyl (H; ●) and ^{11}C-L-deprenyl-D2 (D; ○). Note that maximum value of ordinate for heart, lungs, spleen, liver, and stomach is only half that of kidneys (0.02%/mL vs. 0.04%/mL).

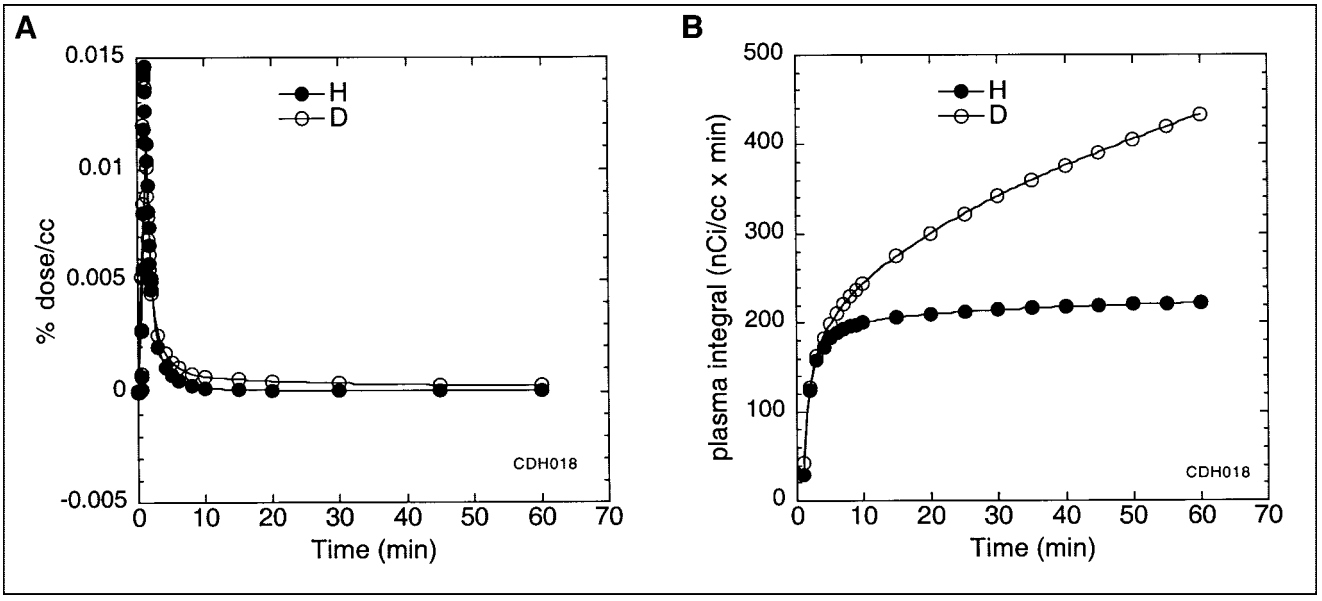

FIGURE 3. (A) Time–activity curves for arterial plasma for ^{11}C-L-deprenyl (H; ●) and ^{11}C-L-deprenyl-D2 (D; ○). (B) Plasma integral for time–activity curves show that value of arterial plasma input function is greater with deuterium-substituted tracer.

of using the IQ parameter rather than λk_3 as an index of MAO B activity because it is dependent on blood flow.

For both ^{11}C-L-deprenyl and ^{11}C-L-deprenyl-D2, the values of λk_3 between the 4 organs are significantly nonhomogeneous ($F_{3,12}$ = 42 for ^{11}C-L-deprenyl-D2 and 100 for ^{11}C-L-deprenyl; $P < 0.0001$). Pairwise comparison was performed using Tukey's method (*33*). We found that all ROI pairs are significantly different except the lungs and spleen. The order of λk_3 is: kidneys ≥ heart >* lungs = spleen (*significantly different using Tukey's test at the familywise error rate of 0.05, 2-sided). A similar analysis for K_1 showed that the value for the heart is significantly smaller than that for the lungs, spleen, and kidney, which are not significantly different from one another.

DISCUSSION

Postmortem studies in humans have reported high MAO B activity in the liver, myocardium, kidney, duodenum, and lung, with very little activity in the spleen (*34*,*35*), and immunohistochemical studies have determined the cellular localization of both MAO A and B in several human tissues outside of the central nervous system (*36*,*37*).

We now report the first results of studies exploring the feasibility of imaging MAO B activity in peripheral organs in healthy human subjects. We patterned these exploratory studies on our use of deuterium-substituted ^{11}C-L-deprenyl as a mechanistic tool for PET studies of MAO B in the human and baboon brain (*23*,*25*). ^{11}C-L-Deprenyl is a sui-

TABLE 1
Values for IQ and Model Terms for ^{11}C-L-Deprenyl (H) and ^{11}C-L-Deprenyl-D2 (D) Calculated Using 3-Compartment Model

Organ	IQ* (mL/min/g)	K_1†	k_2	k_3‡	λk_3*	k_3/k_2‡
Heart (H)	0.43 ± 0.08	0.65 ± 0.13	0.22 ± 0.06	0.49 ± 0.16	1.47 ± 0.41	2.19 ± 0.36
Heart (D)	0.23 ± 0.05	0.65 ± 0.23	0.26 ± 0.05	0.16 ± 0.013	0.39 ± 0.06	0.65 ± 0.14
Lungs (H)	0.095 ± 0.02	2.74 ± 1.60	0.84 ± 0.41	0.14 ± 0.026	0.45 ± 0.093	0.21 ± 0.10
Lungs (D)	0.032 ± 0.0065	2.51 ± 0.72	0.77 ± 0.25	0.042 ± 0.010	0.141 ± 0.036	0.064 ± 0.035
Kidneys (H)	1.06 ± 0.14	2.17 ± 0.32	0.40 ± 0.17	0.48 ± 0.15	2.76 ± 0.34	1.25 ± 0.23
Kidneys (D)	0.4 ± 0.11	1.61 ± 0.22	0.33 ± 0.16	0.11 ± 0.047	0.56 ± 0.13	0.35 ± 0.07
Spleen (H)	0.111 ± 0.012	1.71 ± 0.64	0.44 ± 0.16	0.045 ± 0.007	0.172 ± 0.02	0.112 ± 0.042
Spleen (D)	0.061 ± 0.015	1.93 ± 0.61	0.47 ± 0.13	0.018 ± 0.004	0.072 ± 0.02	0.037 ± 0.007
Liver§ (H)	0.46 ± 0.12					
Liver§ (D)	0.32 ± 0.06					

*D significantly smaller than H ($P < 0.002$).
†Not significant except for kidneys, where K_1 (H) > K_1 (D); $P = 0.04$.
‡D significantly smaller than H ($P < 0.01$).
§Model terms other than IQ could not be calculated for liver.

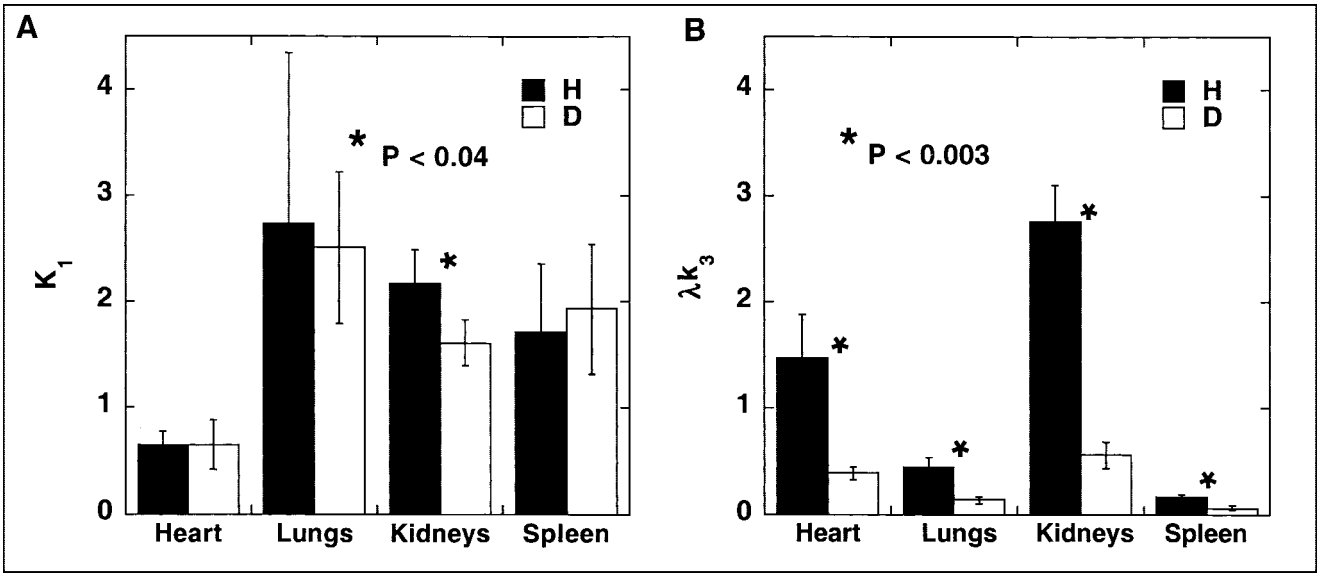

FIGURE 4. (A) Bar graph compares plasma-to-brain transfer function (K_1) for ^{11}C-L-deprenyl (H; ■) and ^{11}C-L-deprenyl-D2 (D; □). (B) Bar graph compares λk_3, which is index of MAO B activity. Note that values for K_1 did not differ except in kidney, which was barely significant ($P < 0.04$) in contrast to λk_3, which showed marked significant reductions in all organs ($P < 0.003$).

cide inactivator of MAO B. It irreversibly inhibits the enzyme by covalently binding to it after being activated by cleavage of the C–H bond on the methylene carbon of the propargyl group. Because a carbon–deuterium bond is more difficult to cleave than a carbon–hydrogen bond, the rate of binding in brain is reduced when ^{11}C-L-deprenyl is substituted with deuterium atoms in the methylene group. Thus, the utilization of the deuterium isotope effect has the potential to identify the specific molecular event in the interaction between the labeled compound and the organ.

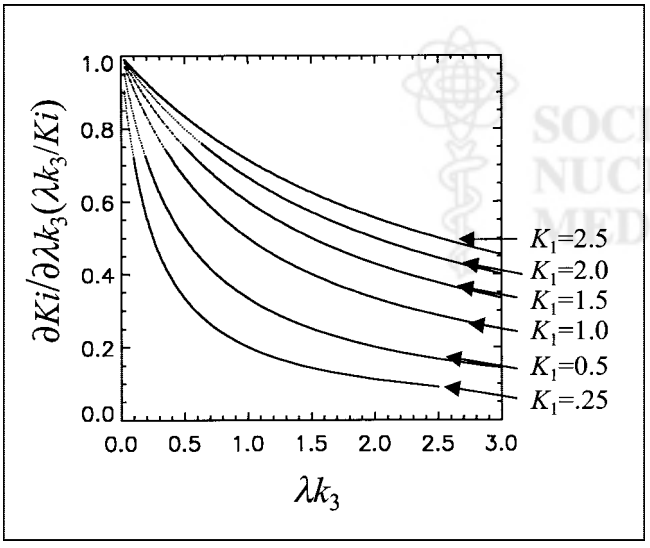

FIGURE 5. Plot of $\partial Ki/\partial \lambda k_3(\lambda k_3/Ki)$ vs. λk_3 for K_1 values of 0.25, 0.50, 1.0, 1.5, 2.0, and 2.5 mL/min/mL. Note that when *Ki* changes very little with relatively large changes in λk_3, uptake is flow limited. With larger values of K_1, *Ki* is sensitive to changes in λk_3 over much wider range than for lower values.

Accordingly, we compared the kinetic patterns of ^{11}C-L-deprenyl/^{11}C-L-deprenyl-D2 pair in different organs in healthy volunteers to determine those in which the rate of binding is reduced by deuterium substitution. The use of the isotope effect rather than a specific MAO B inhibitor drug avoids the confounds of drug-induced changes in other parameters such as blood flow and also avoids potential risks associated with MAO inhibition in healthy subjects. A similar strategy has been used in mechanistic PET studies on the heart with ^{18}F-6-fluorodopamine (*38*) and with ^{11}C-phenylephrine (*39*).

In paired studies comparing ^{11}C-L-deprenyl and ^{11}C-L-deprenyl-D2, the heart, lungs, kidneys, and spleen were unambiguously visualized and each showed a reduction in uptake and reduced values of k_3 and λk_3 with deuterium substitution, indicating that MAO B is responsible for all or part of the organ binding. Moreover, the kinetic pattern indicated that, after an initial rapid influx and clearance, binding is irreversible in these organs.

Irreversibly binding tracers such as ^{11}C-L-deprenyl, which show a rapid rate of binding, are difficult to quantify in organs of high MAO activity because binding can be limited by tracer delivery. Thus, it is important to try to achieve a balance between a sufficiently high binding rate to the molecular target to give a statistically meaningful counting rate in an ROI yet a slow enough binding so that flow is not the rate-limiting step. A high k_3/k_2 ratio indicates a high rate of binding relative to efflux and a potential underestimation of binding. This has been referred to as the flow-limited situation and is illustrated in Figure 5. This applies to some extent to the binding of ^{11}C-L-deprenyl but less for ^{11}C-L-deprenyl-D2 in the kidneys. Deuterium substitution reduces the value of k_3/k_2 by a factor of 3–4 for all organs examined,

demonstrating the advantage of using ^{11}C-L-deprenyl-D2 to quantify MAO B in peripheral organs where the signal represents MAO B. This is similar to our observation that ^{11}C-L-deprenyl-D2 is superior to ^{11}C-L-deprenyl for studies of MAO B in the human brain (*23*).

There are some potentially important differences between the brain and peripheral organs in terms of radiotracer quantification. In the brain, hydrophilic metabolites are normally excluded by the blood–brain barrier. This is not the case in peripheral organs; thus, it is possible that nonspecific binding may dominate the image even in the presence of the specific molecular target such as MAO if an organ serves as a major excretory pathway for labeled metabolites. We were surprised to find that we could use the arterial input function of the parent tracer in our model calculations for the heart, lungs, kidneys, and spleen, indicating that the influx of labeled metabolites did not contribute measurably to the image. However, the pattern in the liver did not change significantly with deuterium substitution and differed from that for other peripheral organs (even though the liver is known to have high MAO B (*34*)), and we were not able to calculate model terms. Although the IQ for the liver shows a 30% reduction due to the fact that the plasma input from ^{11}C-L-deprenyl-D2 is larger than that from ^{11}C-L-deprenyl (Table 1), the inability to calculate model terms indicates that liver clearance may be a pathway for the excretion of labeled metabolites, thereby limiting the use of this method to measure liver MAO B.

We note that there is considerable intersubject variability in the model term λk_3 for the 4 organs. The coefficient of variation expressed as a percentage ranges from 13% to 27% for ^{11}C-L-deprenyl and from 15% to 29% for ^{11}C-L-deprenyl-D2 (Table 1). This is larger than the intersubject variability for brain MAO B. For example, in baseline measures of brain MAO B in healthy individuals with ^{11}C-L-deprenyl-D2 (*28*), the coefficient of variation ranges from 11% to 17%. The factor or factors contributing to the variability in peripheral organ MAO B among individuals is not known.

In organs showing an isotope effect, MAO B activity is greatest in the kidney and the heart with somewhat lower activity in the lung and the spleen. This is the general pattern reported in postmortem studies (*34*) with the exception of the liver (which has been reported to have the highest MAO B activity but which we could not quantify). High kidney MAO B activity is of interest because MAO breaks down filtered dopamine in the kidney (*40*). Kidney dopamine is believed to exert a natriuretic effect through inhibition of different transport systems, including the Na^+-K^+pump, the Na^+H^+ antiporter, and Na^+-P cotransporter.

MAO B activity has been reported to be very high in the human duodenum, presumably serving a protective role in breaking down vasoactive amines present in foods (*11*,*34*). Both ^{11}C-L-deprenyl and ^{11}C-L-deprenyl-D2 showed high accumulation in the gut area. We have not yet performed ROI analysis of the gut area because of the difficulty in organ identification. We did note that the stomach showed high accumulation of radioactivity consistent with the presence of MAO in the stomach (*41*); however, the kinetic patterns for ^{11}C-L-deprenyl versus ^{11}C-L-deprenyl-D2 were different among different individuals. Thus, gut and stomach activity will require further study.

CONCLUSION

We have shown that the deuterium isotope effect is useful in assessing the binding specificity of labeled deprenyl to peripheral MAO B and that MAO B can be visualized and quantified in the heart, lungs, kidneys, and spleen but not the liver. Of the organs in which MAO B can be visualized, MAO B is highest in the kidneys and heart. Quantitation is improved by the use of ^{11}C-L-deprenyl-D2, similar to prior studies on the brain. This study indicates that ^{11}C-L-deprenyl-D2 will be a useful radiotracer for measuring the effects of physiologic variables such as age and disease as well as the effect of therapeutic drugs and tobacco smoke on peripheral MAO B, similar to studies of MAO B inhibitor drugs on the brain. Whole-body MAO B imaging may also be useful in identifying target organs in drug development and in determining drug dosing regimes for therapeutic MAO B inhibitor drugs under development for the treatment of neurodegenerative and other diseases.

ACKNOWLEDGMENTS

The authors are grateful to Robert Carciello, Donald Warner, Payton King, Noelwah Netusil, Bud Jayne, and Pauline Carter for advice and assistance in performing these studies. We are also grateful to the people who volunteered for these studies. This work was performed at Brookhaven National Laboratory under contract DE-AC02-98CH10886 with the U.S. Department of Energy and supported by its Office of Biological and Environmental Research and by National Institutes of Health grant NS 15380.

REFERENCES

1. Shih JC, Chen K, Ridd MJ. Monoamine oxidase: from genes to behavior. *Ann Rev Neurosci.* 1999;22:197–217.
2. Johnston JP. Some observations upon a new inhibitor of monoamine oxidase in brain tissue. *Biochem Pharmacol.* 1968;17:1285–1297.
3. Knoll J, Magyar K. Some puzzling effects of monoamine oxidase inhibitors. *Adv Biochem Psychopharmacol.* 1972;5:393–408.
4. Youdim MDH, Riederer P. Dopamine metabolism and neurotransmission in primate brain in relationship to monoamine oxidase A and B inhibition. *J Neural Transm Suppl.* 1993;91:181–195.
5. Selikoff I, Robitzek E, Ornstein G. Treatment of pulmonary tuberculosis with hydrazide derivatives of isonicotinic acid. *JAMA.* 1952;150:973–980.
6. Zeller EA, Barsky J, Berman ER. Amine oxidases. XI. Inhibition of monoamine oxidase by 1-isonicotinyl-2-isopropylhydrazine. *J Biol Chem.* 1955;214:267–274.
7. Caldecott-Hazard S, Schneider LS. Clinical and biochemical aspects of depressive disorders: III. Treatment and controversies. *Synapse.* 1992;10:141–168.
8. Parkinson's Study Group. Effect of deprenyl on the progression of disability in early Parkinson's disease. *N Engl J Med.* 1989;321:1364–1371.
9. Sano M, Ernesto C, Thomas RG, et al. A controlled trial of selegiline, alpha tocopherol or both as the treatment of Alzheimer's disease. *N Engl J Med.* 1997;336:1216–1222.
10. Mannelli M, Pupilli C, Lanzillotti R, et al. Catecholamines and blood pressure regulation. *Hormone Res.* 1990;34:156–160.

11. Kopin I. Monoamine oxidase (MAO): relationship to foods, poisons, and medicines. *Biog Amines.* 1993;9:355–365.
12. Vindis C, Seguelas MH, Lanier S, et al. Dopamine induces ERK activation in renal tubule epithelial cells through H_2O_2 produced by monoamine oxidase. *Kidney Int.* 2001;59:76–86.
13. Cohen G, Kesler N. Monoamine oxidase and mitochondrial respiration. *J Neurochem.* 1999;73:2310–2315.
14. Langston JW, Irwin I, Langston EB, et al. Pargyline prevents MPTP-induced parkinsonism in primates. *Science.* 1984;225:1480–1483.
15. Inoue H, Castagnoli K, Van Der Schyf C, et al. Species-dependent differences in monoamine oxidase A and B-catalyzed oxidation of various C4 substituted 1-methyl-4-phenyl-1,2,3,6-tetrahydropyridinyl derivatives. *J Pharmacol Exp Ther.* 1999;291:856–864.
16. Kalaria RN, Harik SI. Blood-brain barrier monoamine oxidase: enzyme characterization in cerebral microvessels and other tissues from six mammalian species, including human. *J Neurochem.* 1987;49:856–864.
17. Fowler JS, MacGregor RR, Wolf AP, et al. Mapping human brain monoamine oxidase A and B with ^{11}C-suicide inactivators and positron emission tomography. *Science.* 1987;235:481–485.
18. Fowler JS, Volkow ND, Wang GJ, et al. Brain MAO A inhibition in cigarette smokers. *Proc Natl Acad Sci USA.* 1996;93:14065–14069.
19. Fowler JS, Wang G-J, Volkow ND, et al. Inhibition of monoamine oxidase B in the brains of smokers. *Nature.* 1996;379:733–736.
20. Fowler JS, Volkow ND, Wang, G-J, et al. Age-related increases in brain MAO B in healthy human subjects. *Neurobiol Aging.* 1997;18:431–435.
21. Fowler JS, Volkow ND, Logan J, et al. Monoamine oxidase B (MAO B) inhibitor therapy in Parkinson's disease: the degree and reversibility of human brain MAO B inhibition by Ro 19 6327. *Neurology.* 1993;43:1984–1993.
22. Belleau B, Moran J. Deuterium isotope effects in relation to the chemical mechanism of monoamine oxidase. *Ann NY Acad Sci.* 1963;107:822–839.
23. Fowler JS, Wang G-J, Logan J, et al. Selective reduction of radiotracer trapping by deuterium substitution: comparison of [^{11}C]L-deprenyl and [^{11}C]L-deprenyl-D2 for MAO B mapping. *J Nucl Med.* 1995;36:1255–1262.
24. MacGregor RR, Fowler JS, Wolf AP. Synthesis of suicide inhibitors of monoamine oxidase: carbon-11 labeled clorgyline, L-deprenyl and D-deprenyl. *J Labelled Cmpds Radiopharm.* 1988;XXV:1–9.
25. Fowler JS, Wolf AP, MacGregor RR, et al., Mechanistic positron emission tomography studies: demonstration of a deuterium isotope effect in the MAO catalyzed binding of [^{11}C]L-deprenyl in living baboon brain. *J Neurochem.* 1988;51:1524–1534.
26. Alexoff DL, Shea C, Fowler JS, et al. Plasma input function determination for PET using a commercial laboratory robot. *Nucl Med Biol.* 1995;22:893–904.
27. Dean D, Herbener TE. *Cross-Sectional Human Anatomy*. Philadelphia, PA: Lippincott Williams & Wilkins; 2000:8–59.
28. Logan J, Fowler JS, Volkow ND, et al. Reproducibility of repeated measures of deuterium substituted [^{11}C]L-deprenyl ([^{11}C]L-deprenyl-D2) binding in the human brain. *Nucl Med Biol.* 2000;27:43–49.
29. Logan J, Dewey SL, Wolf AP, et al. Effects of endogenous dopamine on measures of [^{18}F]N-methylspiroperidol binding in the basal ganglia: comparison of simulations and experimental results from PET studies in baboons. *Synapse.* 1991;9:195–207.
30. International Commission on Radiological Protection. *Report of the Task Group on Reference Man*. No. 23. New York, NY: Pergamon Press; 1975.
31. Visser TJ, Waarde AV, van der Mark TW, et al. Detection of muscarinic receptors in the human lung using PET. *J Nucl Med.* 1999;40:1270–1276.
32. Patlak CS, Blasberg RG, Fenstermacher JD. Graphical evaluation of blood-to-brain transfer constants from multiple-time uptake data. *J Cereb Blood Flow Metab.* 1983;3:1–7.
33. Tukey JW. Comparing individual means in the analysis of variance. *Biometrics.* 1949;5:99–114.
34. Saura J, Nadal E, van den Berg B, et al. Localization of monoamine oxidases in human peripheral tissues. *Life Sci.* 1996;59:1341–1349.
35. Rodriguez MJ, Saura J, Billet E, et al. MAO A and MAO B localization in human lung and spleen. *Neurobiology.* 2000;8:243–248.
36. Rodriguez MJ, Saura J, Billet EE, et al. Cellular localization of monoamine oxidase A and B in human tissues outside of the central nervous system. *Cell Tissue Res.* 2001;304:215–220.
37. Rodriguez MJ, Saura J, Finch CC, et al. Localization of monoamine oxidase A and B in human pancreas, thyroid and adrenal glands. *J Histochem Cytochem.* 2000;48:147–151.
38. Ding Y-S, Fowler JS, Gatley SJ, et al. Mechanistic PET studies of 6-[^{18}F]fluorodopamine in living baboon heart: selective imaging and control of radiotracer metabolism using the deuterium isotope effect. *J Neurochem.* 1995;65:682–690.
39. Raffel DM, Corbett JR, del Rosario RB, et al. Sensitivity of [^{11}C]phenylephrine kinetics to monoamine oxidase activity in normal human heart. *J Nucl Med.* 1999;40:232–238.
40. Pizzinat N, Remaury A, Parini A. The renal monoamine oxidases: pathophysiology and targets for therapeutic intervention. *Curr Opin Nephrol Hypertens.* 1998;7:33–36.
41. Odegaard S, Borkje B, Skagen DW, et al. Enzyme activities in human gastric mucosa in gastritis and resected stomachs. *Scand J Gastroenterol.* 1986;21:1257–1264.